JOURNAL OF AEROSPACE COMPUTING, INFORMATION, AND COMMUNICATION
Vol. 5, October 2008

Multi-Sensor-Based Fully Autonomous Non-Cooperative Collision Avoidance System for Unmanned Air Vehicles

Giancarmine Fasano* , Domenico Accardo† , and Antonio Moccia‡
University of Naples "Federico II", Naples, NA, I80125, Italy

and
Ciro Carbone§ , Umberto Ciniglio¶ , Federico Corraro# , and Salvatore Luongo**
Italian Aerospace Research Center (CIRA), Capua, CE, I81043, Italy

DOI: 10.2514/1.35145

This paper presents a fully autonomous multi-sensor anti-collision system for Unmanned Aerial Vehicles. This system is being developed by the Italian Aerospace Research Center in collaboration with the Department of Aerospace Engineering of the University of Naples "Federico II". The research project is entitled TECVOL and is funded in the frame of the National Aerospace Research Program. The system prototype will be initially installed onboard a manned laboratory aircraft equipped for automatic control, therefore flight tests will verify the adequacy of attained performances for supporting fully autonomous flight. The obstacle detection and tracking function is performed by a multi-sensor configuration made up by a pulsed Ka-band radar, two visible (panchromatic and color) video cameras, two infrared video cameras, and two computers. One computer is dedicated to real time sensor fusion and communication with the radar and the flight control computer (by means of a deterministic data bus), the other is devoted to image processing. On the basis of the tracking estimates and of a Collision Avoidance Software, the flight control computer generates and follows in real-time a proper escape trajectory. In order to evaluate the performance of the collision avoidance system, numerical simulations have been performed taking into account the obstacle detection sensors' accuracy, unmanned aircraft's and intruder's flight dynamics, navigation system accuracy and latencies, and collision avoidance logic. The relevant results helped to assess overall system performances and are discussed in depth.

Nomenclature

$\vec{r}$	relative position between aircraft with Autonomous Collision Avoidance module and intruder
t	time

Received 15 October 2007; accepted for publication 16 January 2008.

* PhD Researcher, Department of Aerospace Engineering, g.fasano@unina.it, P.le Tecchio 80, I80125, Naples, Italy.
† Assistant Professor, Department of Aerospace Engineering, daccardo@unina.it, P.le Tecchio 80, I80125, Naples, Italy, AIAA Senior member.
‡ Full Professor, Department of Aerospace Engineering, antonio.moccia@unina.it, P.le Tecchio 80, I80125, Naples, Italy, AIAA Senior member
§ PhD Researcher, Flight Systems Department, c.carbone@cira.it, Via Maiorise, I81043, Capua (CE), Italy
¶ Senior Researcher, Flight Systems Department, u.ciniglio@cira.it, Via Maiorise, I81043, Capua (CE), Italy
# Senior Researcher, Flight Systems Department, f.corraro@cira.it, Via Maiorise, I81043, Capua (CE), Italy
** Researcher, Flight Systems Department, s.luongo@cira.it, Via Maiorise, I81043, Capua (CE), Italy

Nomenclature

D	Maximum Deviation of aircraft with Autonomous Collision Avoidance from its nominal trajectory
S	Minimum Separation Distance between aircraft with Autonomous Collision Avoidance module and intruder safety bubble
$\vec{P}_A$, $\vec{P}_B$	positions of aircraft with Autonomous Collision Avoidance module and intruder
R	safety bubble radius
T_S	sampling time
$\vec{V}_A$, $\vec{V}_B$	velocities of aircraft with Autonomous Collision Avoidance module and intruder
$\vec{V}_{AB}$	relative velocity vector
γ_A, γ_B	slope angles of aircraft with Autonomous Collision Avoidance module and intruder
χ_A, χ_B	track angles of aircraft with Autonomous Collision Avoidance module and intruder
ϕ_M	extreme roll angle for *Maximum Command Control Strategy*
Ψ	intruder azimuth
Θ	intruder elevation

I. Introduction

IN recent years, worldwide research for integration of Unmanned Aerial Vehicles (UAVs) in Civil Airspace has increased considerably [1–4]. Several organizations for the development of standards were involved in writing the guidelines to allow UAVs a safe access to flight [5,6]. Among other prescriptions, an onboard system for autonomous obstacle Detect, Sense and Avoid (DS&A) was considered mandatory to attain equivalent levels of safety to manned aircrafts.

At present, UAV autonomous anti-collision systems are at an experimental level [7,8] and research studies are still being carried out to find system requirements and sensing solutions. In general, different sensing architectures have been selected, and the trend is to develop a customized Obstacle DS&A system for each UAV platform [9]. In this framework, multi-sensor fusion is considered a valuable tool.

The Italian Aerospace Research Center (CIRA) planned to develop a High Altitude, Long Endurance (HALE) UAV for civil applications (P.R.O.R.A. UAV Program). Within this program, the TECVOL project aims at developing the technologies needed to support the HALE UAV flight autonomy, and will develop a hardware/software prototype integrating the following functions:

- Autonomous Flight Path Execution
- Autonomous Approach and Landing
- Obstacle DS&A
- Autonomous Runway Search and Lock and
- Enhanced Remote Piloting.

In the TECVOL preliminary studies [10], a multi-sensor configuration was designed to perform the obstacle detection and tracking function on the basis of the assigned sensing requirements. It is comprised of a pulsed Ka-band radar, four electro-optical (EO) sensors, and two processing units, one of which is dedicated to communication with the flight control computer. The functional and hardware architecture of the DS&A System are described in detail in the following sections.

The autonomous collision avoidance module is based on two core algorithms. Firstly, a customized multisensor tracking software ensures that intruders' dynamics is properly followed and estimated. Secondly, a decision making logic has been developed to handle collision conditions in real time and perform adequate evasive maneuvers.

The detection and tracking system was tested in several computer simulated collision scenarios, which were designed taking into account UAV and intruder flight dynamics. Furthermore, simulated obstacle and navigation measures were generated by means of documented models of the sensors.

In this paper the overall tracking accuracy is evaluated combining estimates relative to all the considered scenarios. Preliminary numerical results show the different performances obtained depending on the tracking phase and the reference frame where the intruder position is estimated. Collision Avoidance strategies are discussed including the two main functions of Collision Detection and Conflict Resolution. The Collision Detection decision-making flow

chart is also presented and discussed. Moreover, the Conflict Resolution strategy based on minimum displacement from original trajectory is detailed and compared with other collision avoidance strategies.

Finally, planned flight tests are briefly described and they will include sessions where a single intruder enters the Field of Regard (FOR) of DS&A sensors. Initial tests will verify the capability of the designed system to detect and track the intruder by integrating the measurements of Microwave and EO sensors. Subsequently, real Collision Avoidance tests will be performed.

II. Collision Avoidance Problem Definition

A. Geometric Formulation

Several approaches to the problem of collision avoidance have been adopted in literature. It is worthwhile noting that most of the proposed methods are not suitable for real-time applications, because of the non-deterministic computational time needed for making a decision. A comprehensive survey of these methods is provided in Ref. 11.

Generally speaking, *Autonomous Collision Avoidance* (ACA) decision-making can be formulated as a two stage process. Firstly, *Conflict Detection*, a potential conflict between two aircrafts will be detected, determining if the future positions, after a certain amount of time should experience a loss of minimum separation. In such a case the trajectory of aircraft A/C_A has to be re-planned by solving a *Conflict Resolution* problem.

Conflict detection and resolution processes have been addressed in a 3D environment using information of current positions and instantaneous speed vectors, on the basis of geometric methods. Figure 1 outlines the geometry which has been adopted for a collision situation between two aircrafts in the 3D North-East-Down (NED) reference frame: consider the aircraft with ACA module on-board (A/C_A) modeled as a point object—with 3 Degree Of Freedom (DOF)—and velocity $\vec{V}_A$, while the other aircraft (A/C_B, considered as an intruder) is modeled as a sphere with radius R (safety bubble) having velocity $\vec{V}_B$.

B. System Requirements

All requirements for the obstacle detection system were estimated by following a line of reasoning as described in a previous work [10]. The focus was on mid-air flight and thus assumed maximum approaching speed was 500 kts. The all-time all-weather requirement was also considered. In its initial configuration TECVOL aims at demonstrating the capability to avoid one non cooperative flying obstacle in the search volume. In the final configuration the system should be able to avoid up to four obstacles.

Table 1 reports the assigned sensing requirements. It is worth noting that they comply with international standards [5,6].

Furthermore the Aircraft Collision Avoidance system discussed in this paper must be:

REQ_1 Autonomous: no pilots onboard

REQ_2 Safe: a miss distance of 500 ft must always be guaranteed

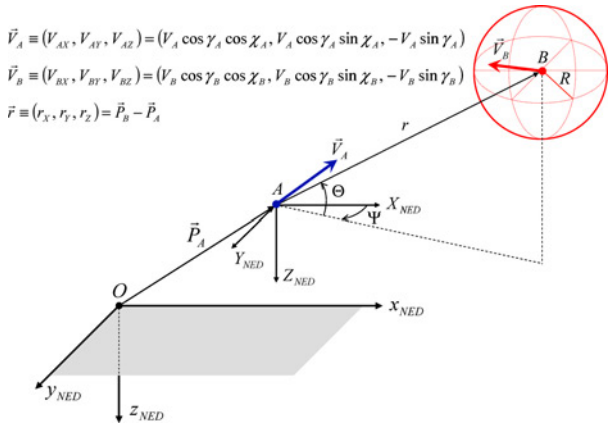

Fig. 1 Collision geometry between a point of mass A and a sphere B with radius R.

Table 1 Sensing system requirements

Parameter	Value
Field of regard extent in azimuth	$-110°/+110°$
Field of regard extent in elevation	$-15°/+15°$
Range resolution	20m
Azimuth resolution	0.27°
Elevation resolution	0.27°
Data rate	10 Hz

REQ_3 Nuisance Free: a maneuver has to be started only in case of a real threat

REQ_4 At Minimum Deviation: the deviation from the nominal trajectory, as a consequence of a collision avoidance maneuver, has to be minimized.

III. Obstacle Detection, Tracking, and Collision Avoidance System

A. Functional Architecture

Figure 2 outlines the ACA module within the closed-loop control system. Its core is represented by a decision-making algorithm, having as an input the speed and the position of the intruder ($\vec{P}_B$, $\vec{V}_B$) and of the own aircraft ($\vec{P}_A$, $\vec{V}_A$). The outputs of the decision making algorithm are reference signals to the autopilot, in terms of demanded speed module (V_d), slope angle (γ_d) and track angle (χ_d).

B. Hardware Architecture

The hardware configuration is made up of:

- a pulsed Ka-band radar
- two visible (panchromatic and color) video cameras having the same field of view (FOV). The color camera was selected for obstacle identification, which will be tested in the second part of TECVOL project and is not covered in this paper
- two infrared (IR) video cameras to increase IR FOV
- two computers, one dedicated to sensor fusion and communication with the flight control computer and with the radar, the other devoted to image processing
- a set of navigation sensors (Attitude and Heading Reference System, Laser Altimeter, Standalone GPS, and Air Data Sensor)
- a Guidance, Navigation and Control (GNC) Computer capable of processing in real time obstacle dynamics and UAV navigation data to generate escape trajectories and the relevant commands for servos and
- a CAN bus that performs deterministic data handling.

Figure 3 depicts the various components and the relevant data-links. The selected configuration demonstrates the DS&A capability in a reduced field of regard (120° in azimuth).

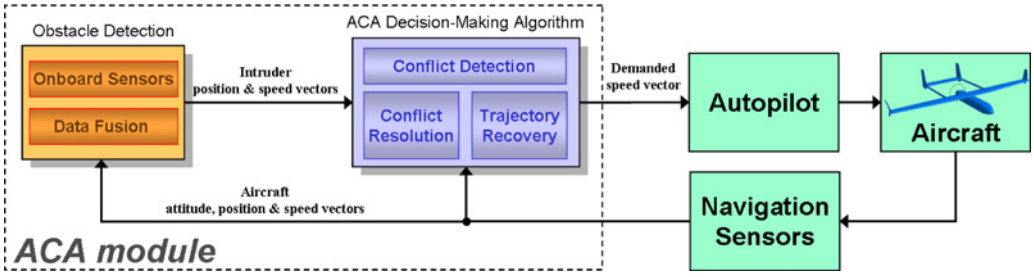

Fig. 2 ACA system functional architecture within the closed-loop control system.

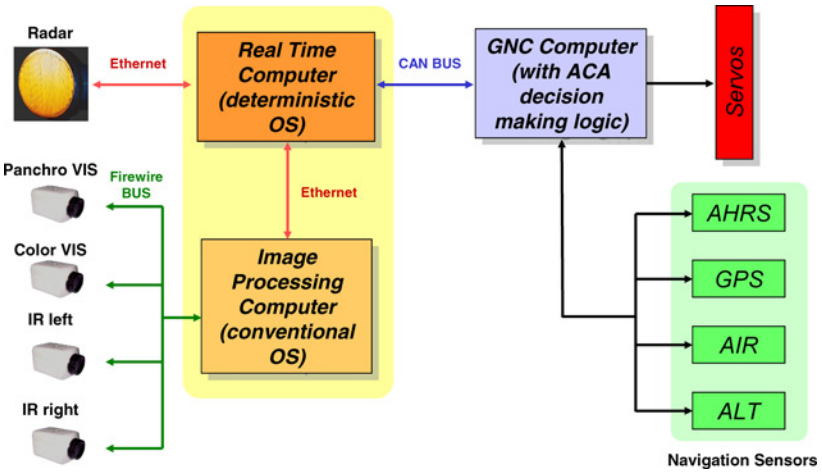

Fig. 3 DS&A/GNC hardware architecture.

IV. Detailed Software Design

Developed software components can be divided in following three classes:

– multi-sensor detection and tracking algorithms
– decision-making collision avoidance algorithms and
– software developed to evaluate system performance in a realistic simulation environment.

A. Sensor Fusion Algorithm for Obstacle Detection and Tracking

The logical architecture of the complete sensor fusion algorithm for flying obstacles detection and tracking is outlined in Figure 4 and was described in detail in Ref. 12.

The multi-sensor tracking algorithm is a key element of the DS&A system. In fact, the system is completely autonomous, and thus it is mandatory to have reliable estimates not only of intruders' positions, but also of their motion, as the latter information is needed by the collision avoidance logic to decide whether or not it is necessary to perform an evasive maneuver.

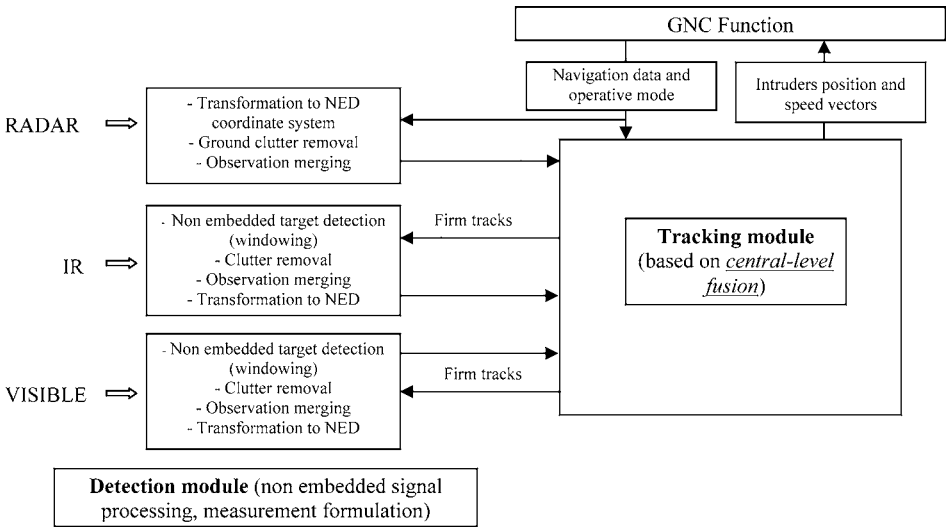

Fig. 4 Logical architecture of obstacle detection and tracking system.

In the considered case, tracking logic has been designed taking into account the particular features of civil airspace scenarios. These scenarios are primarily characterized by the very low probability of a dense multi-target environment. Of course, depending on the sensors' angular accuracy and detection range, different flying obstacles could produce miscorrelation though respecting the bubble distance. However, this potentially occurs over large distances, when avoidance maneuvers are not initiated considering a nuisance-free approach. Another aspect to be taken into account is that the most important quality parameter of the tracker is its reliability at short distances rather than its absolute accuracy since this is the most critical situation for the entire system.

On the basis of these concepts, available solutions in the choice of coordinate systems and filtering schemes were analyzed in a previous work [12]. In particular, three different filtering options were tested and compared in a simplified quasi-collision scenario, such as linear Kalman filter in cartesian converted coordinates [13], three almost independent filters in spherical coordinates [14], and extended Kalman filter (EKF) in cartesian coordinates. All three filtering schemes exhibited satisfying performances with respect to system requirements; however EKF was demonstrated to be the best compromise between accuracy and reliability at very short ranges. Therefore, it has been selected for real time implementation and it is described in this paper.

The state vector is supposed to be made up by nine components, which are the obstacle coordinates in NED (North-East-Down reference frame with origin in the aircraft center of mass) with their first and second time derivatives. A classical Singer model is assumed for the three acceleration components [15]. The model is flexible since it allows to change the filter bandwidth by adjusting input parameters in order to account for different dynamic environments. In the EKF implementation the relation state vector-measurements is linearized at each time step on the basis of the latest state estimate. It is worth noting that EKF allows for simple track update also with angular measures only (EO sensors).

System data rate is 10 Hz, which is consistent with the obstacle detection requirements illustrated in a previous section. Moreover, navigation data are used by the algorithm at the same frequency so that UAV dynamics is properly followed during tracking phase without an excessive computational load.

As mentioned earlier, tracking algorithm operates in NED reference frame. This refers not only to the filtering/prediction phase but also to gating and track/measurement correlation. Sensor measurements (both radar and EO) must be converted to NED before being used, therefore they are corrupted by the error in the attitude angles evaluation. As a consequence, tracking performance is closely correlated to the navigation system, and measurement covariance matrix in the Kalman filter must be corrected to account for this additional noise to keep its consistency. It is worth noting that performing tracking directly in the Body Reference Frame (BRF) with origin in the aircraft center of mass and axes along longitudinal, lateral and vertical aircraft axes, attitude angles' errors are avoided but acceleration and angular velocity measurements (with their errors) must be used in any case. Moreover, the relative motion in the BRF includes attitude dynamics, unlike its projection in NED, which makes it more difficult to track.

Since it is not possible to eliminate navigation errors, it is important to estimate their effects on tracking accuracy. In the following, the effects of navigation errors on tracking accuracy are examined and an analysis of the errors both in BRF and in NED estimates is proposed. In particular, tracking output is supposed to be made up of estimates of range, range rate, azimuth and elevation in BRF with their time derivatives, and azimuth and elevation in NED (the so called stabilized azimuth and stabilized elevation [14]) with their time derivatives.

B. Decision-Making Collision Avoidance Algorithm

The *ACA Decision-Making Algorithm* module, shown in Fig. 2, implements the high-level state diagram of Fig. 5.

The initial state (nominal state) is "Conflict Detection": in this state the collision avoidance algorithm continuously checks, with sampling time T_S, if a potential conflict can occur. In such a case (i.e., event ⟨*Conflict detected*⟩ happens) a "Conflict Resolution" maneuver has to be planned and performed, until conflict has not been resolved (event ⟨*Conflict resolved*⟩). When this occurs, the state "Nominal Trajectory Recovery" is reached and a maneuver to recovery the original nominal trajectory is started. Of course, in this state the detection of potential collisions is always in progress since the intruder could change its direction in unpredictable way.

State "Blind Avoidance Maneuver" has been added to manage the possibility that the intruder goes out of Field Of Regard (FOR). When this state is reached (event ⟨*Intruder outside FOR*⟩) intruder's trajectory is estimated by a proper propagation of the last measured speed vector.

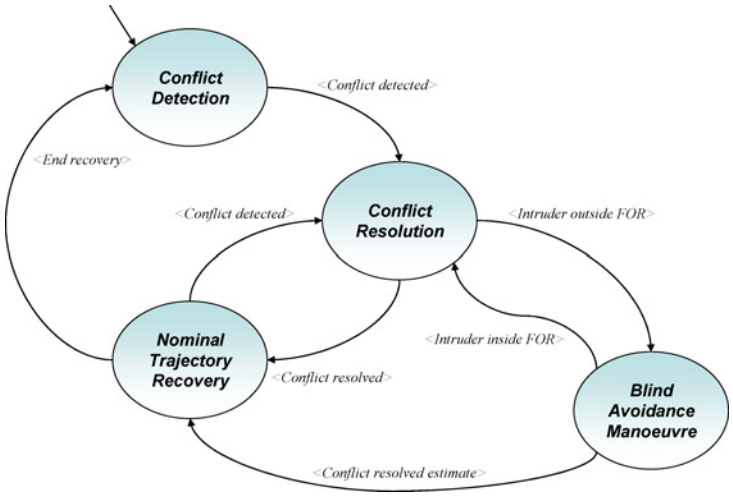

Fig. 5 Decision-making collision avoidance state machine.

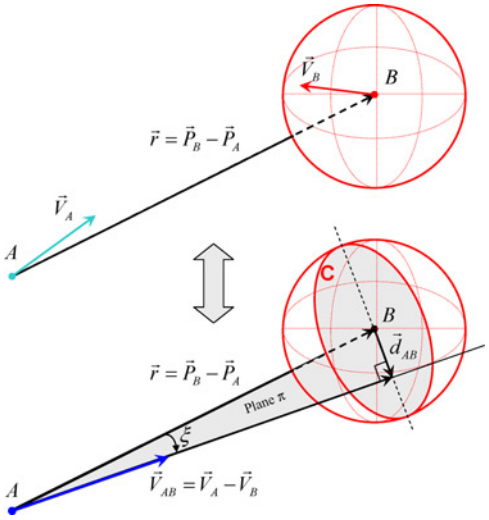

Fig. 6 Definition of *minimum separation distance* vector $\mathbf{d_{AB}}$.

Conflict detection phase is based on the fact that the relative velocity vector $\vec{V}_{AB} = \vec{V}_A - \vec{V}_B$ transforms the kinematic collision avoidance problem – where both aircrafts are moving – into an equivalent problem where aircraft A/C_B is stationary (the sphere) and point object A moves with relative velocity $\vec{V}_{AB}$ with respect to it (see Figure 6).

Let $\vec{d}_{AB}$ be a vector defined in Ref. 13 as the *minimum separation distance* experienced between aircraft, after a certain time horizon. It can be calculated as follows (see Fig. 6):

$$\vec{d}_{AB} = \frac{\vec{r} \cdot \vec{V}_{AB}}{\|\vec{V}_{AB}\|^2} \vec{V}_{AB} - \vec{r} \tag{1}$$

It is shown in Ref. 16 that if a point object A and a sphere B with radius R are moving in a 3D environment with constant velocity vectors, respectively $\vec{V}_A$ and $\vec{V}_B$, they are headed for a collision if and only if the following conditions are satisfied (Conflict Detection conditions):

$$\|\vec{d}_{AB}\| \leqslant R \text{ and } \dot{r} < 0 \tag{2}$$

Thanks to the necessary and sufficient condition (2), REQ_3 is satisfied. The Conflict Resolution strategy proposed in this paper, called *Minimum Deviation* control strategy, is based on the analytical solution of the following kinematic optimization problem: *find the minimum change in nominal trajectory of aircraft A to be forced (compatible with its envelope limitation and dynamic constraints) in order to avoid a collision with the safety bubble surrounding aircraft B.*

Let $\vec{P}_A(t) = [x_A(t), y_A(t), z_A(t)]^T$ and $\vec{P}_B(t)$ be, respectively, A/C$_\mathrm{A}$ and A/C$_\mathrm{B}$ nominal trajectories. $\vec{P}_A(t)$ can be expressed in terms of velocity vector $\vec{V}_A(t)$ along the nominal trajectory as follows:

$$\vec{P}_A(t) = \vec{P}_A(t_0) + \int_{t_0}^{t} \vec{V}_A(\tau) d\tau \tag{3}$$

Let $\vec{P}_A^d(t)$ be the modified trajectory resulting from the demanded velocity vector function $\bar{V}_A^d(t) \equiv \bar{V}_A^d(V_A^d, \chi_A^d, \gamma_A^d, t)$. The deviation from the nominal trajectory of aircraft A is:

$$\vec{P}_A^d(t) - \vec{P}_A(t) = \int_{t_0}^{t} \left[\vec{V}_A^d(\tau) - \vec{V}_A(\tau)\right] d\tau \tag{4}$$

Minimizing nominal trajectory deviation—under envelope limitation and dynamic constraints—means minimizing the quantity $\|\Delta\vec{P}_A(t)\| = \|\int_{t_0}^{t} \Delta\vec{V}_A(\tau)d\tau\|$ as stated by the following nonlinear programming problem:

$$\min_{V_A^d, \chi_A^d, \gamma_A^d} \left\| \int_{t_0}^{t} \Delta\vec{V}_A(\tau) d\tau \right\|$$

$$s.t. \begin{cases} \left\| \vec{P}_A^d(t) - \vec{P}_B(t) \right\| \geqslant R, \quad \forall t \geqslant t_0 \\ V_A^d(t) \in [V_{A\min}, V_{A\max}],\ \gamma_A^d(t) \in [\gamma_{A\min}, \gamma_{A\max}] \\ \exists t_a^A > 0 \end{cases} \tag{5}$$

Constraint (5)-1,

$$\left\| \vec{P}_A^d(t) - \vec{P}_B(t) \right\| = \left\| \vec{r}(t) + \int_{t_0}^{t} \Delta\vec{V}_A(\tau) d\tau \right\| \geqslant R$$

ensures that minimum separation distance R is never violated (Collision Avoidance); constraint (5)–2 represents the aircraft envelope limitations; (5)–3 is a dynamic constraint, since the closed-loop system "Aircraft & Autopilot" has a finite settling time t_a^A for velocity vector changes, i.e., $\vec{V}_A^d$ cannot be reached instantaneously but requires a certain time t_a^A. In order to approach analytically the general Collision Avoidance problem (5), three assumptions are hereafter considered:

1) change in velocity vector occurs only at time t_0, i.e., $\Delta\vec{V}_A(t)$ is a step function [17]
2) straight aircraft trajectories at constant speeds and
3) no aircraft envelope limitations and dynamic constraints.

General problem (5), under assumptions (1)–(3), becomes

$$\min_{V_A^d, \chi_A^d, \gamma_A^d} \left\| \Delta\vec{V}_A \right\|$$

$$s.t. \left\| \vec{d}_{AB}^{\,d} \right\| = R \tag{6}$$

It is possible to prove that this new problem admits an analytical solution, as follows

$$\vec{V}_A^d = \frac{V_{AB}\cos(\eta - \xi)}{\sin\xi} \left[\sin\eta \cdot \hat{V}_{AB} - \sin(\eta - \xi) \cdot \hat{r}\right] + \vec{V}_B. \tag{7}$$

where $\hat{r}$ and $\hat{V}_{AB}$ are respectively the unit vectors of $\vec{r}$ and $\vec{V}_{AB}$; moreover, $\eta = \sin^{-1}\frac{R}{\|\vec{r}\|}$ and it has the same sign of ξ, angle formed by vectors $\vec{r}$and $\vec{V}_{AB}$. General problem (5) has been simplified thus the minimization of A/C$_\mathrm{A}$

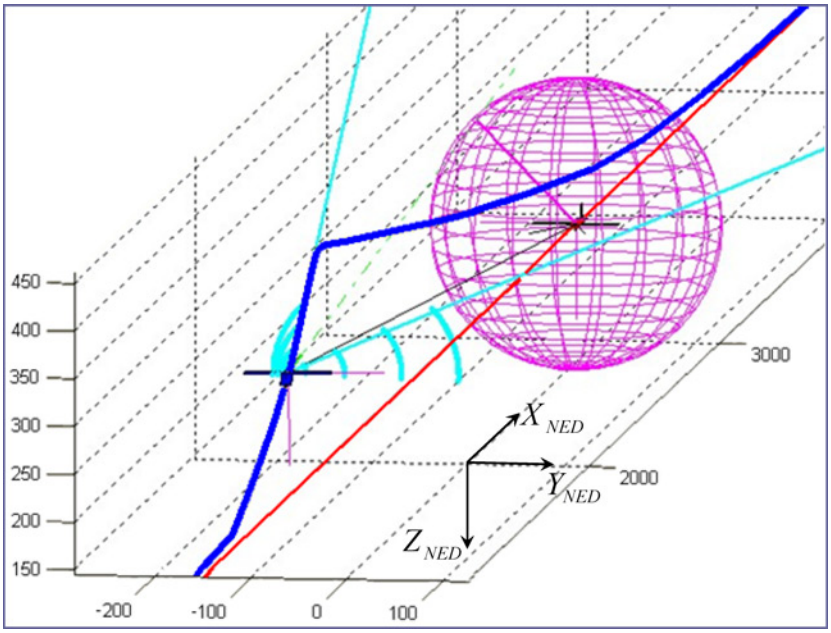

Fig. 7 Conflict resolution: a 3D collision avoidance maneuvers.

nominal trajectory deviation has been made equivalent to the minimization of vector $\Delta\vec{V}_A$. This new problem admits analytical solution (7) to the collision avoidance problem and does not require the resolution of any numerical optimization problem, thus resulting suitable for real-time applications. Afterwards, assumptions 1)–3) have been removed, in order to take into account envelope limitation and dynamic constraints expressed in problem (5). This analytical solution works by continuously changing the aircraft speed vector (with 10 Hz update rate) with the aim of skimming the safety bubble surrounding the intruder. As outlined in expression (7), collision avoidance manoeuvres are performed in 3D (Fig. 7), by changing simultaneously aircraft speed module, track and slope angles. This is a noticeable improvement with respect to available collision avoidance systems. For instance, TCAS only suggests to the pilot maneuvers into the vertical plane in cooperation with the other aircraft.

C. Simulation Software Environment

Besides run-time algorithms, a set of software tools needed to assess system performance in a realistic simulation environment have been developed.

The development process of ACA algorithms foresees the following phases:

- Methodology Selection and Numerical Evaluation
- Detailed Design, Implementation and Off-Line Verification
- On Ground Experimental Validation and
- In-Flight Demonstration Testing.

This paper deals only with the results achieved during the first two design steps. In particular, the off-line numerical validation of the designed algorithms has been performed by using an unstructured synthetic simulation environment. This includes the aircraft 6DOF dynamic behavior with related aerodynamic and inertial uncertainties, the detailed models of both navigation and situational awareness sensors, the outside environment with Von-Karman turbulence and wind-shear models, and flying obstacle trajectories generated randomly by using a Montecarlo approach.

Regarding obstacle detection sensors it is supposed to have a pulse radar (no Doppler speed measurement), and an EO system. Radar range accuracy is 15 m (rms), and its angular accuracy is 2° (rms) both in elevation and in azimuth, data rate is 1 Hz. The radar Field Of View (FOV) dimensions are 120° in azimuth and 20° in elevation, whereas the EO FOV is supposed to be 50° in azimuth and 40° in elevation. These values are consistent with the specifications of the sensors selected for flight tests. The radar detection process has been simulated by computing

probability of detection for the target as a function of its range from the UAV [18,19] and performing Monte-Carlo statistical simulations. In particular, in view of planned flight tests, the intruder has been simulated as a Swerling 2 target (propeller-driven airplane) [18] with a mean Radar Cross Section of 1 m^2. As for the EO sensors parameters, it has been supposed that the EO system gives angular measures with an accuracy of 0.1° (in the BRF) at a frequency of 2 Hz, when intruder distance is less than 3 km. EO sensors usually work at higher frequencies, nevertheless a low frequency was chosen to account for the time necessary for image processing. Moreover, a large improvement of tracking performance is obtained even at this frequency.

Sensors' mounting misalignment error has been neglected. However, a calibration phase is foreseen before the first collision avoidance flight tests and has already been positively tested, showing the capability to estimate cameras' alignment with respect to the AHRS with a residual error in the order of 0.1°. Furthermore, cameras' vibration has been neglected due to the fact that EO images taken during first preliminary flights devoted to system identification and functional verification have shown that image quality is not affected by these phenomena.

V. Numerical Validation of Algorithms

A. Obstacle Detection and Tracking

Obstacle detection and tracking performance has been tested using the previously described software tools and following the line of reasoning shown in Fig. 8.

Ten scenarios have been generated by considering quasi-collision initial trajectories and the execution of different avoidance maneuvers. The adopted Collision Avoidance algorithm is described in Ref. 16 and represents a preliminary version of the Minimum Deviation Control Strategy outlined in this paper. In particular, simulated maneuvers differ in the plane where they are executed (vertical or horizontal) and in the strategy (minimum deviation from planned trajectory or maximum control). For example, Fig. 9 shows a horizontal maneuver performed to avoid collision after a sudden change of direction by the intruder (scenario 5).

Due to the non deterministic nature of sensor detection, both for radar and EO cameras, a statistical approach is needed to assess algorithm performance. Thus, for each scenario 100 Monte Carlo simulations have been performed regarding the generation of radar and EO measures, and then tracking filters have been applied to their output. In summary, a set of 1000 complete detection/tracking simulations have been performed.

In all the considered scenarios, initial range is of about 6 km. As a consequence, for the given radar parameters, probability of detection is high and there are very few detection misses. Thus, after the first intruder detection, the system fast switches from tentative radar tracking to firm radar tracking. On the basis of how EO sensors have been simulated, this tracking phase lasts until the obstacle goes out of the sensors FOV or the distance between the UAV and the intruder becomes smaller than 3 km.

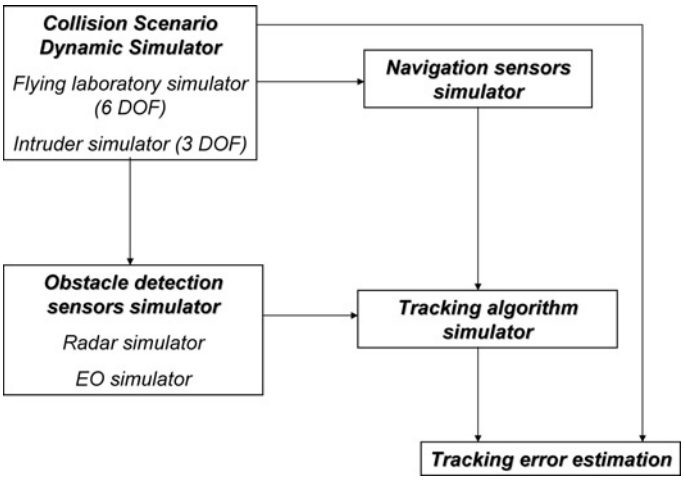

Fig. 8 Logic of tracking performance estimation.

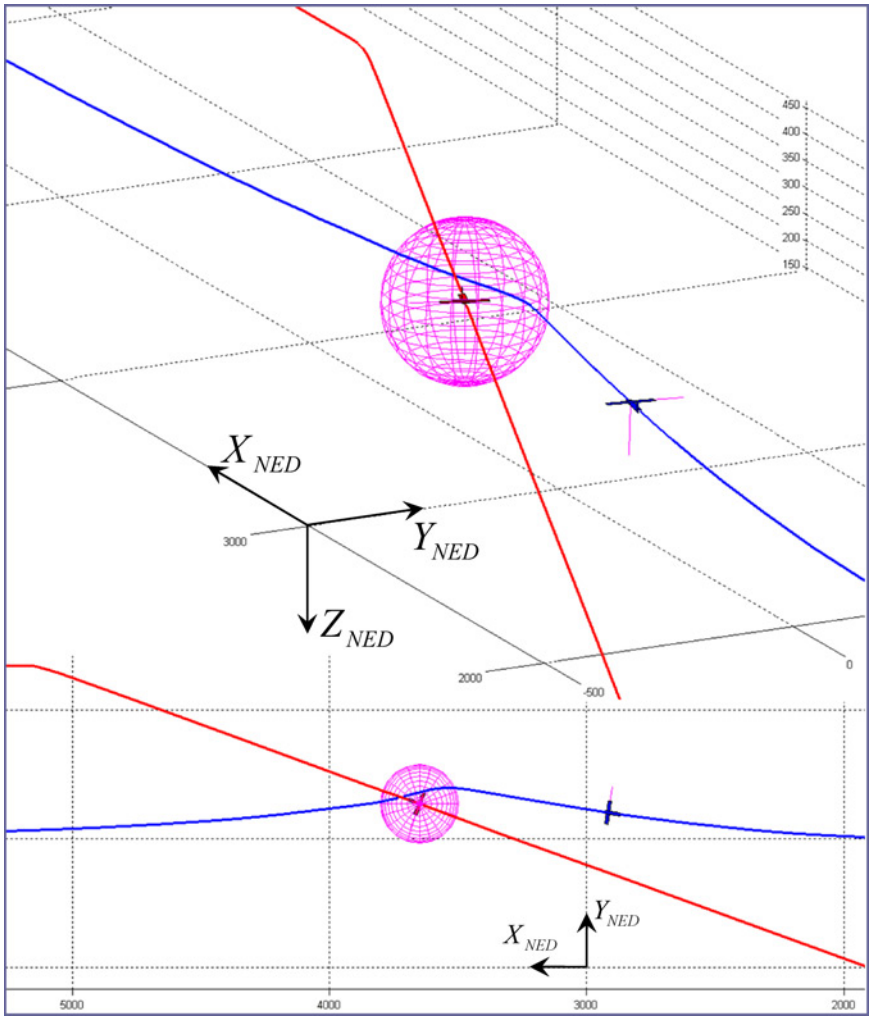

Fig. 9 Graphical description of scenario no. 5.

If this is the case, the system switches to combined radar/EO tracking with a dramatic improvement in angular accuracy, as it is shown in the following. In all cases tracking ends when the intruder is no more detectable by radar/EO sensors because it is out of the FOV. When this happens, after a few seconds the track is lost.

It is worth pointing out that since tracking filter is based on a linear dynamic model in Cartesian NED coordinates, and the intruder follows a straight trajectory, even when the obstacle is no more detectable the accuracy of obstacle positioning is very stable for many seconds. Of course, in real time implementation these estimates will not be used.

In the following, for the sake of brevity only one collision scenario will be examined in detail. Then, statistic data of the simulations performed on all the scenarios will be provided.

However, the performed simulations for the different scenarios and avoidance maneuvers held very similar results in tracking performance, showing that tracking algorithm is robust with respect to UAV flight dynamics and collision avoidance maneuver choice. Furthermore, this is also due to the fact that the obstacle is tracked mostly before the avoidance maneuver and in the first few seconds after maneuver initiation. Then, the execution of avoidance maneuver, both because of trajectory and attitude modification, brings the obstacle outside the FOV of the sensors, which are of course body fixed. However, visibility time for both radar and EO sensors does depend on the avoidance strategy, and is longer for minimum deviation maneuvers.

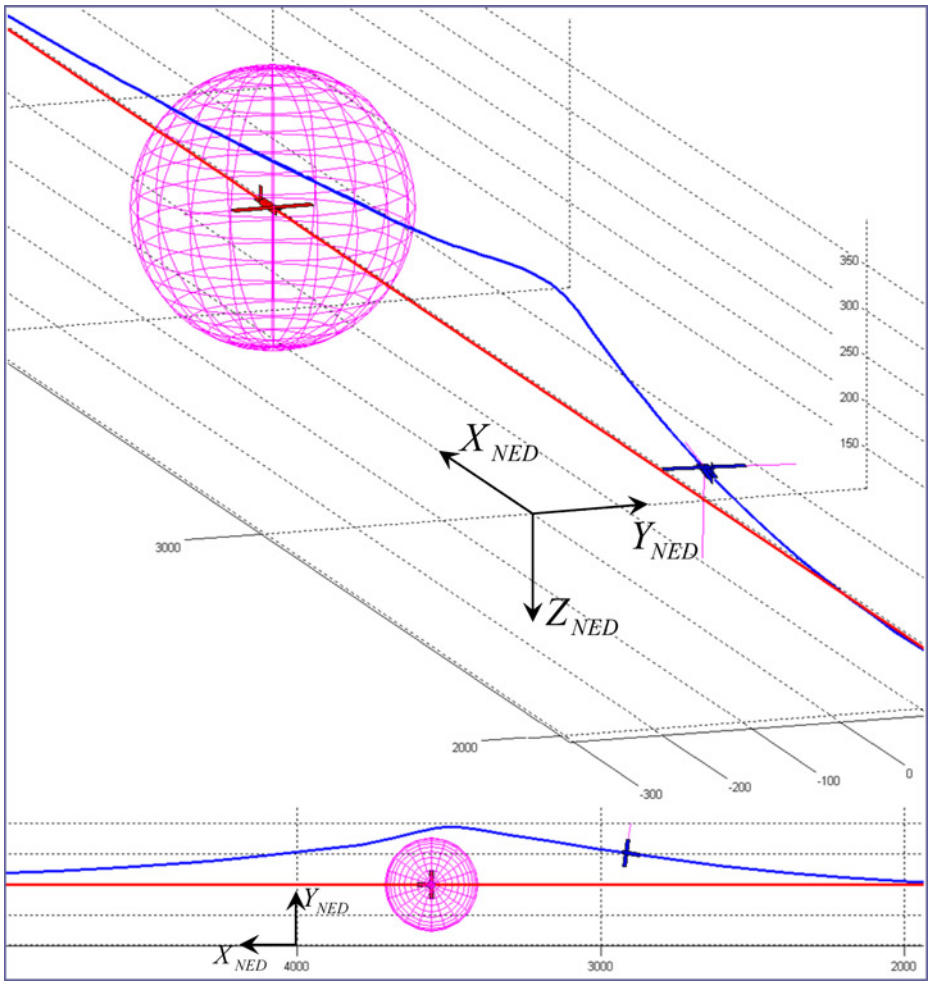

Fig. 10 Scenario considered for detailed analysis.

The considered scenario for detailed analysis is outlined in Fig. 10. The two airplanes fly at an altitude of 300 m, the initial distance among them is 3.5 nm and they are moving towards each other. The UAV avoids collision by means of a maneuver in horizontal plane near the safety bubble.

Exact values for range, azimuth, and elevation with respect to the radar sensor are provided in Figs. 11, 12, and 13. It can be seen that the minimum distance between the airplanes is of about 165 m, and that the intruder goes out of the radar FOV after a time of approximately 70 s.

It is worth noting that the radar is the main sensor and it is the only sensor used for association and track status definition. This also means that EO detection does not influence track status but only track update in terms of state and covariance estimate.

Figure 13 shows that elevation dynamics in body is very perturbed following in substance UAV pitch dynamics. In fact, relative dynamics in NED is much less perturbed, as shown by the trend of stabilized elevation, reported in Fig. 14.

Focusing now on tracking estimates, let us consider first of all tracking performance in a single simulation. Figures 15 and 16 report errors with respect to exact values in range and in azimuth (in BRF). Tracking error (sampled at 10 Hz) is reported in blue, whereas radar error (sampled at 1 Hz) is reported in red.

It can be seen how the algorithm filters sensor noise though preserving its reliability, in fact no biases are produced. EO sensors detection corresponds in the simulated scenario to a time of about 39 s. Since cameras provide only angular

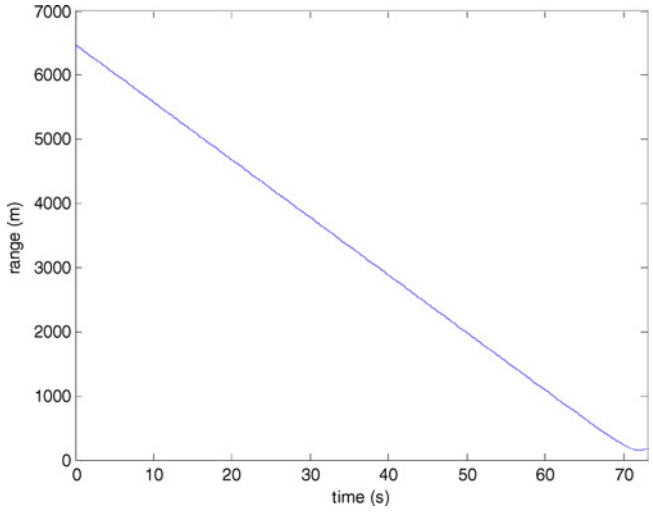

Fig. 11 Range in the considered scenario as a function of time.

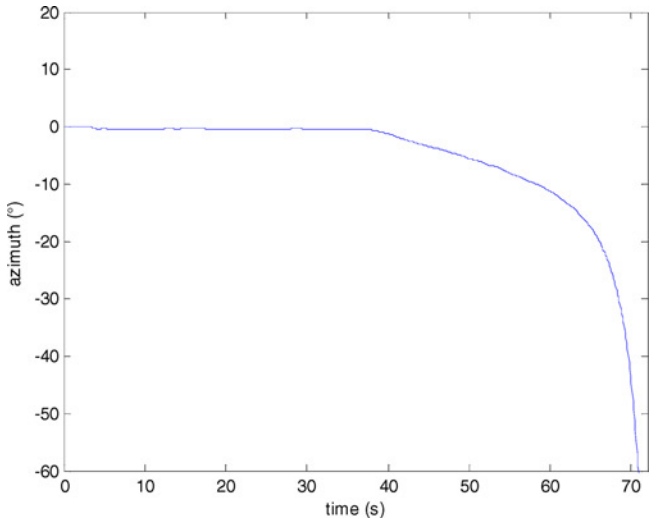

Fig. 12 Azimuth (in BRF) in the considered scenario as a function of time.

measures, their effect on range error is not so much evident, though an improvement can be observed and is due to the coupling between range and angles produced by the Cartesian EKF structure. EO effect can be better appreciated in Fig. 16, with a large improvement in tracking accuracy. It is worth pointing out that the more "perturbed" trend of azimuth estimates with respect to the range ones is due to the UAV attitude dynamics more than on the tracker (which operates in NED, as stated before).

The following figures report range and angular errors for the considered scenario as a function of time, considering all the 100 MonteCarlo simulations and the statistical mean and standard deviation calculated on them. The different tracking phases (firm radar and firm radar/EO) are explicitly indicated. During firm radar tracking phase, the tracker follows intruder trajectory with a positioning accuracy which improves in time due in substance to the reducing distance between the airplanes. EO detection is not so much visible in range error diagram (Fig. 17), whereas it reduces so much standard deviation of errors on the angles that the three diagrams (mean, mean plus standard deviation, mean minus standard deviation) are hard to distinguish (Fig. 18 and Fig. 19). If we consider NED estimates

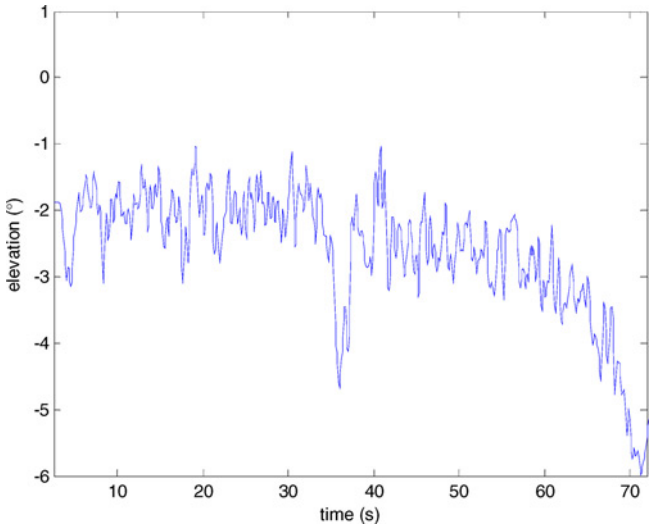

Fig. 13 Elevation (in BRF) in the considered scenario as a function of time.

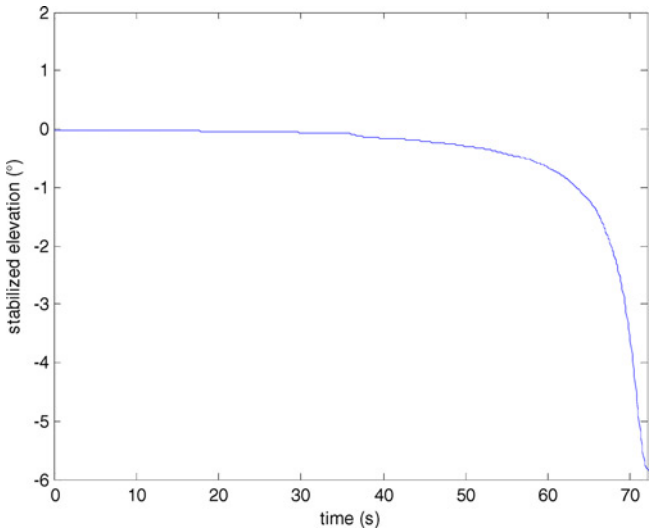

Fig. 14 Stabilized elevation in the considered scenario as a function of time.

(Figs. 20 and 21), then a less perturbed trend is obtained (no effects of attitude dynamics) and it is easier to estimate reduction of standard deviation in angular errors. Furthermore, it is interesting to observe that biases are produced both in stabilized azimuth and in stabilized elevation. This is closely connected to the AHRS errors in estimating attitude angles. In fact, stabilized azimuth error mean equals in substance the bias in heading estimate, whereas a smaller error mean is observed on stabilized elevation, which is of the same order of magnitude of biases in estimates of roll and pitch angles. These relations are due to the fact that an almost non maneuvering flight segment is considered. In summary, biases in navigation errors are almost completely filtered in body angular estimates, and thus corrupt only NED estimates.

It is also interesting to point out that, regarding the accuracy of gating operation [20], no track loss phenomena have been observed in all the performed simulations.

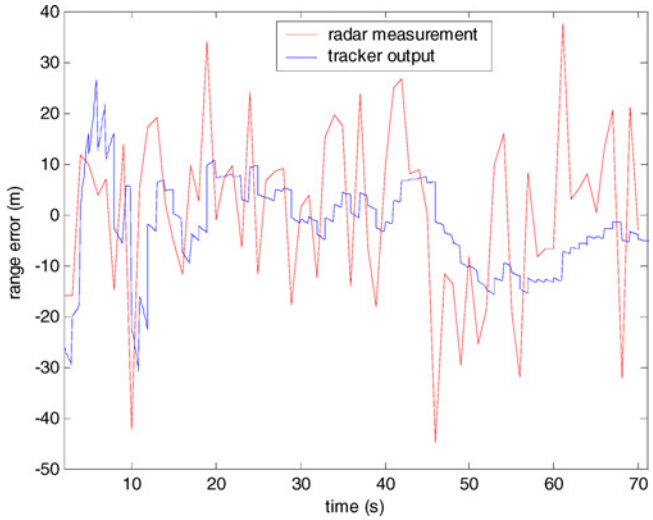

Fig. 15 Radar and track range error.

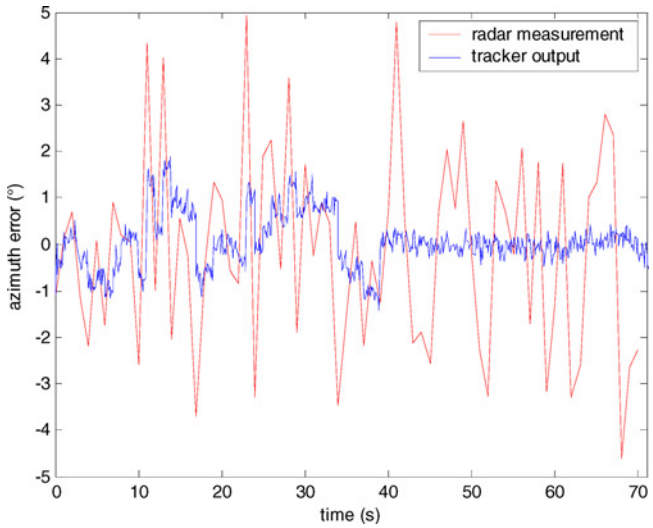

Fig. 16 Radar and track azimuth error.

Final synthetic results for all the 10 scenarios are reported in Tables 2 and 3. In particular, Table 2 reports time averaged values of statistical mean errors for all the scenarios and the different estimates, whereas Table 3 reports time averaged values of statistical standard deviations for the different errors.

It can be observed that a small bias in range error is generated in firm radar/EO tracking. This is due to the fact that because of track update with EO cameras measurements, track covariance reduces and so also the weight of radar range measurements does. Nevertheless, RMS error reduces in firm radar/EO phase also in range estimate.

Finally, it is worth noting that standard deviations in angular errors do not depend on the considered reference frame, because the origin of the variability is in both cases in the radar/EO detection process. This fact results also in the presented diagrams.

In summary, it can be concluded that developed hardware/software for obstacle detection and tracking is compliant with the requirements indicated in the preliminary studies of TECVOL project.

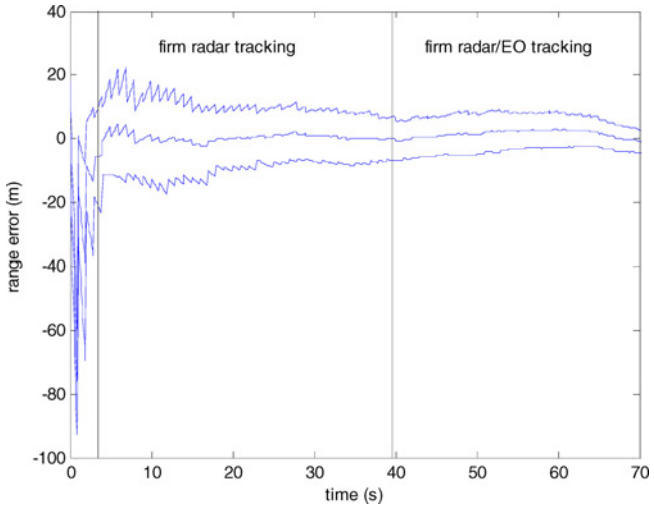

Fig. 17 Error in range estimate, in terms of mean and standard deviation.

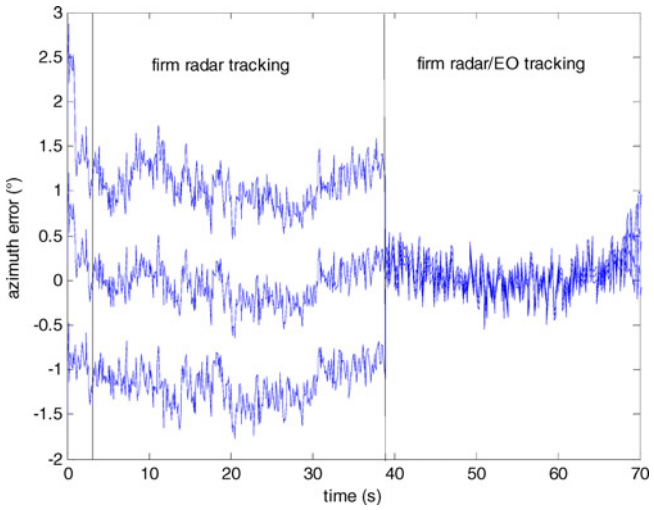

Fig. 18 Error in azimuth estimate, in terms of mean and standard deviation.

B. Collision Avoidance

Algorithm validation has been carried out via numerical simulations, by defining proper collision scenarios, as shown in Fig. 22. These test scenarios have been designed according to standard specification given in Ref. 6. It is assumed that onboard detection sensors can search from $\pm 110°$ in azimuth and $\pm 15°$ in elevation [3], as required in Table 1.

In each conflict scenario it is assumed that intruder speed vector is initially constant and such that a collision will certainly happen: Fig. 22 shows—for a given intruder (A/C_B) initial position—a "cone" of speed vectors that guarantee a collision with A/C_A, if a collision avoidance maneuver is not performed.

The proposed scenario foresees 4000 starting points (r, Ψ, Θ) for the intruder, chosen in a random way, with uniform distribution: $\Psi \sim U[-110°, 110°]$, $\Theta \sim U[-15°, 15°]$.

Simulations have been carried out under the following hypotheses:

1) safety bubble radius: $R = 152.4$ m (500 ft)
2) on-board navigation sensors have been considered with a realistic uncertainty model

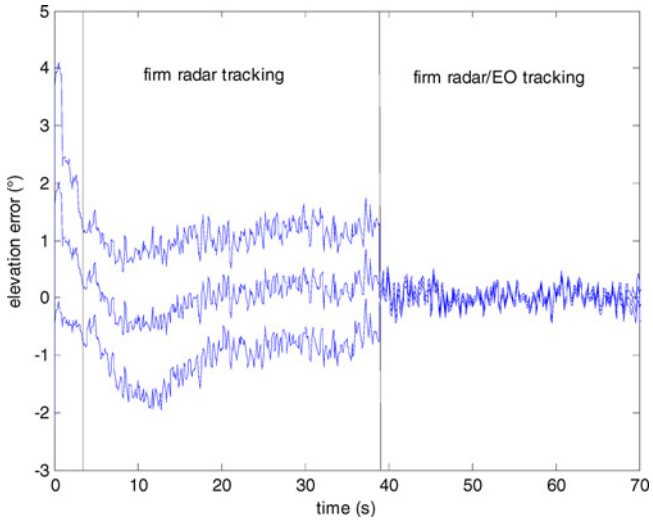

Fig. 19 Error in elevation estimate, in terms of mean and standard deviation.

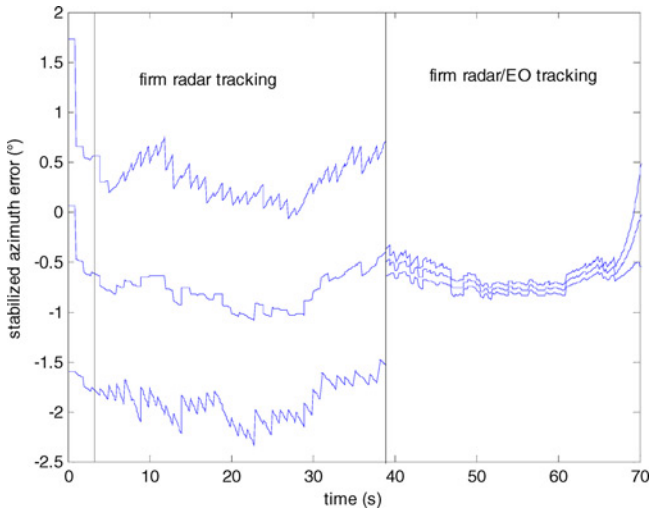

Fig. 20 Error in stabilized azimuth estimate, in terms of mean and standard deviation.

3) on-board detection sensors can search from $\pm 110°$ in azimuth and $\pm 15°$ in elevation (Field Of Regard, FOR).
4) A/C_A is a civil transport aircraft, described by a detailed 6DOF model, flying at speed module constant: $V_A = 250$ kts
5) A/C_B (Civil Transport) has a random speed vector: after time $t_B \sim U[0\,s, 5\,s]$, A/C_B changes randomly its track angle of $\Delta\chi_B \sim U[-20°, 20°]$; moreover, $V_B \sim U[250\,\text{kts}, 500\,\text{kts}]$, $r = 5$ n mi (initial range).

Figure 23 shows performance indexes defined to evaluate ACA algorithms:

– $\mathbf{S} = \min(r(t) - R)$—**Minimum separation distance** between aircraft A/C_A trajectory and the safety bubble of aircraft A/C_B. S < 0 means collision.
– $\mathbf{D} = \max(|d(t)|)$—**Maximum deviation** of aircraft A/C_A from its nominal trajectory, representing the distance to cover in order to return on the nominal trajectory, as a consequence of the avoidance manoeuvre.

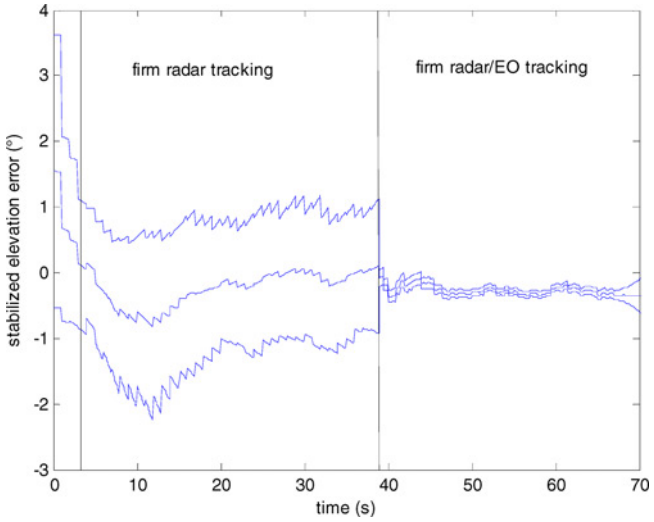

Fig. 21 Error in stabilized elevation estimate, in terms of mean and standard deviation.

Table 2 Mean errors for the available tracking modes

Mean errors	Range (m)	Range rate (m/s)	Azimuth BODY (°)	Azimuth NED (°)	Elevation BODY (°)	Elevation NED (°)
Firm radar tracking	−0.24	0.76	−0.02	−0.75	0.03	−0.21
Firm radar/EO tracking	1.54	0.35	0.07	−0.64	0.02	−0.23

Table 3 Standard deviation of errors for the available tracking modes

Standard deviation of errors	Range (m)	Range rate (m/s)	Azimuth BODY (°)	Azimuth NED (°)	Elevation BODY (°)	Elevation NED (°)
Firm radar tracking	10.30	3.03	1.11	1.10	1.09	1.09
Firm radar/EO tracking	5.90	0.47	0.085	0.085	0.071	0.071

In the sequel, *Minimum Deviation* control strategy will be compared with two classical collision avoidance strategies [21,22], namely *Maximum Command* and *Bang-Bang*, reminded hereafter:

- *Maximum Command Control Strategy*—The control command is a discrete roll angle change, which can assume only three values: $-\phi_M$, 0, $+\phi_M$. The decision is taken once, before starting an avoidance maneuver. Maneuvers are performed in the horizontal plane.
- *Bang-Bang Control Strategy*—The only difference with the previous strategy is that the control command is evaluated here with each sample time, during the avoidance maneuver.

Performance indexes S and D have been computed in each scenario for all algorithms. Figure 24 shows performance index S for Maximum Command, Bang-Bang, and Minimum Deviation strategies. Each point corresponds to a specific scenario and represents S, i.e. the difference between the minimum distance of the aircraft trajectory from the safety bubble and R (safety bubble radius). $S < 0$ means collision. Minimum Deviation strategy is the only one which guarantees no collisions in the considered scenarios, whereas for Maximum Command and Bang-Bang strategies 10 collisions have been observed.

Collision cases found with Maximum Command and Bang-Bang strategies have been analyzed one by one. They are caused by aircraft aggressive maneuvers: because of FOR limitations, when A/C_A starts an avoidance maneuver at maximum roll angle, the probability that intruder exits the FOR is very high; once intruder view is lost, every direction change can not be detected anymore.

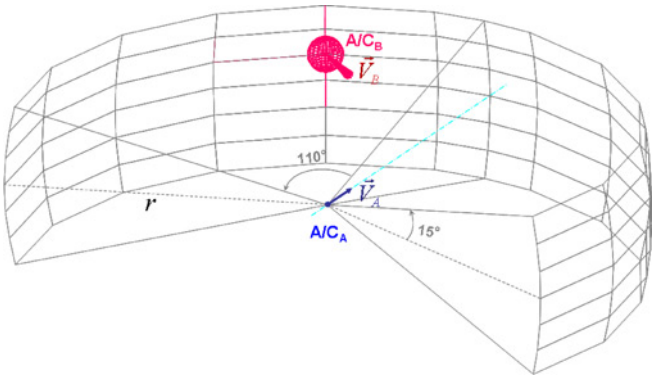

Fig. 22 3D test scenarios definition.

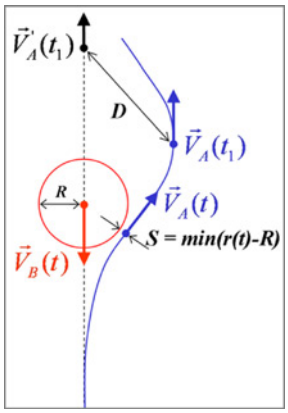

Fig. 23 Performance indexes: S, D.

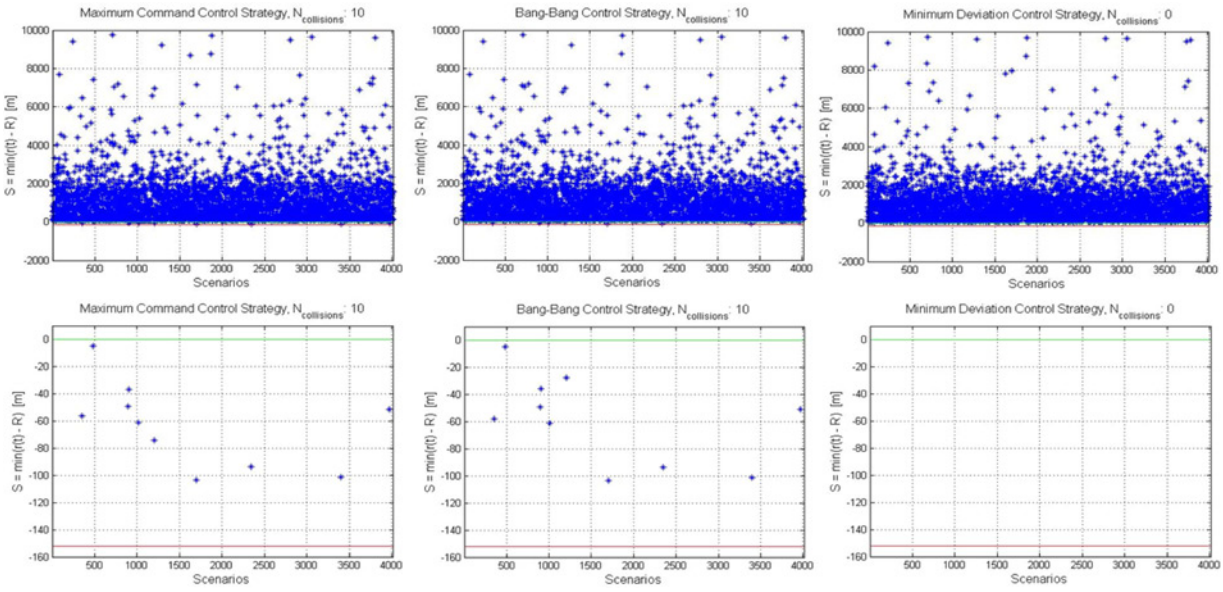

Fig. 24 Minimum separation distance S.

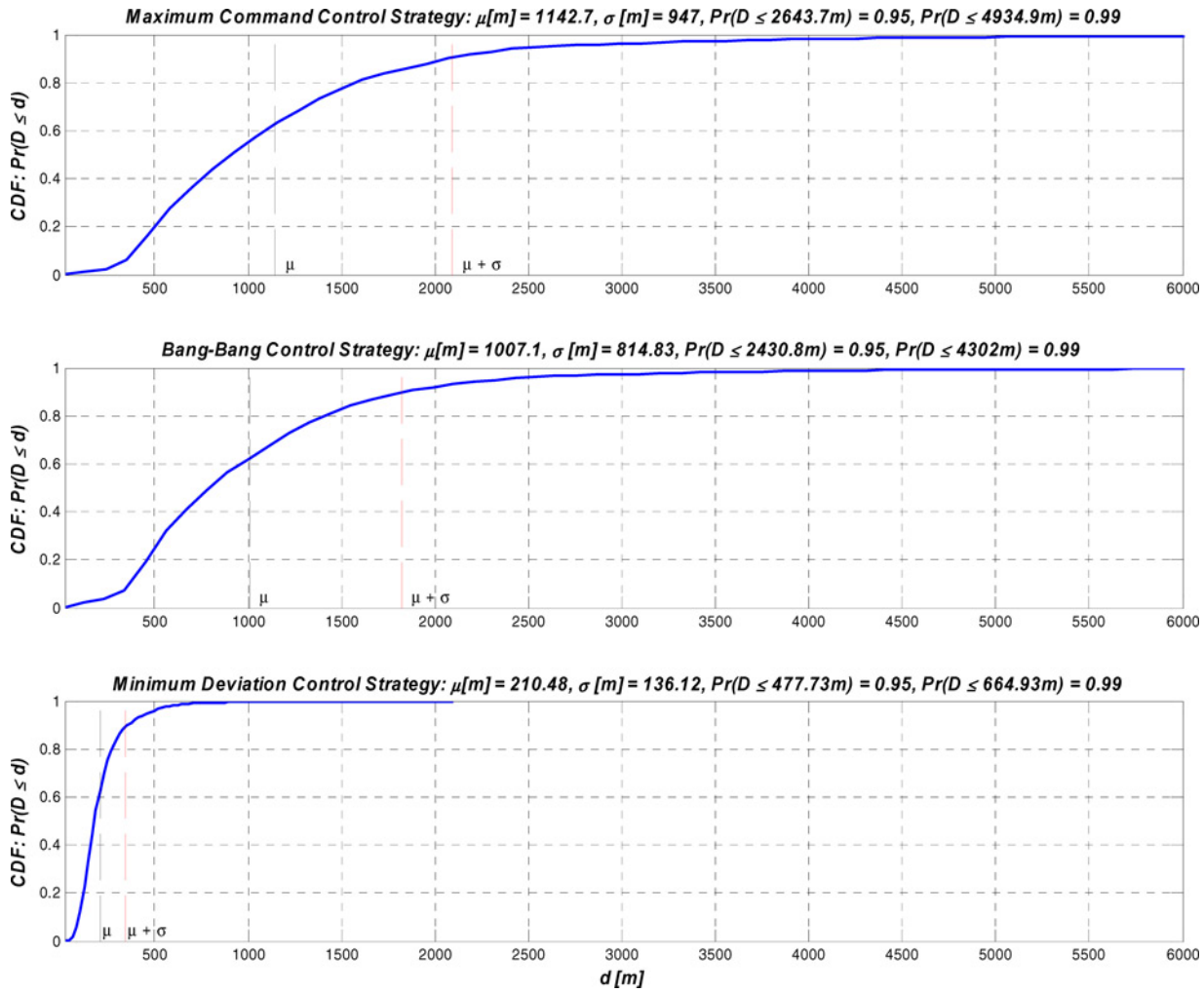

Fig. 25 Cumulative Distribution Function (CDF) associated with random variable D (Maximum Deviation from the nominal trajectory).

Minimum Deviation control strategy is the only one that satisfies REQ_2 in the proposed scenario ($S \geqslant 0$); moreover it offers the advantage of reducing the maximum deviation D from the nominal trajectory (REQ_4), as shown in Figure 25 and Table 4. Several simulation sessions have shown that, for this control strategy, D is about an order of magnitude (mean and standard deviation) less than values obtained with Maximum Command and Bang-Bang control strategies. The combination of these results makes the Minimum Deviation control strategy suitable

Table 4 Performance index D: comparison of control strategies

	Maximum Command Control Strategy	Bang-Bang Control Strategy	Minimum Deviation Control Strategy
Mean μ[m]	1142.7	1007.1	210.48
Std. Dev. σ[m]	947	814.83	136.12
d_1[m]: $Pr(D \leqslant d_1) = 0.95$	2643.7	2430.8	477.73
d_2[m]: $Pr(D \leqslant d_2) = 0.99$	4934.9	4302	664.93
D_{max} [m]	11470	11020	2100

for the integration within the present Air Traffic Management (ATM) system and within an Innovative Future Air Transport System (e.g., IFATS) since it is able to guarantee safety by minimizing the deviation from the original flight plan in a 4D sense (Fig. 25).

VI. System Testing Strategy

Demonstration of hardware and software technologies for Sense and Avoid will be performed in a few months in collision avoidance flight tests. However, a lot of real time hardware-in-the-loop ground tests are already being executed in order to test system behavior and latencies. This section clarifies all these tests and the logic of their design.

Ground tests regard hardware real time capability and communication among the different computing units. Many tests have been performed to verify CAN bus reliability and performance, since latency in data exchange between the flight control computer and the real time computer (see hardware architecture Fig. 3) plays a key role for the sense and avoid function. Though the average data rate is of the order of only one tenth of CAN bus throughput (1 Mbps), data are transmitted in burst mode at a frequency of 10 Hz and the bus has to solve collision phenomena between packets. All the performed tests confirmed CAN reliability, since no loss of messages were observed. Furthermore, it was observed that by introducing appropriate time lags while sending messages (of less than 1 ms) it is possible to reduce latencies up to a few ms.

Complete hardware-in-the-loop tests are currently in progress. In these tests all the onboard and ground systems are activated, together with a radar hardware simulator and all the cameras. Results will be presented in future works.

As for flight tests, they are divided in two main categories: obstacle detection and tracking flight performance assessment, combined autonomous collision avoidance.

In the first category automatic control will not be activated. In particular, in the first tests the flying laboratory will follow an intruder aircraft at higher altitude to keep it in its field of regard for a long time without safety problems (Fig. 26-1). This will enable to verify tracking capabilities with different sets of sensors activated. Intruder at higher altitude will reduce problems due to land clutter.

Then, the flying laboratory will fly several “near collision” “quasi frontal” trajectories with an intruder again at higher altitude (Fig. 26-2). Finally, the same tests will be conducted with the intruder at lower altitude, which is the hardest situation for the necessity to remove land clutter (Fig. 26-3).

Tests will be repeated for several weather and illumination conditions.

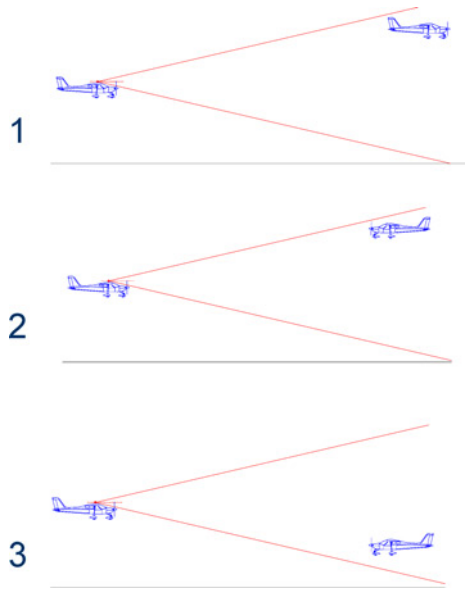

Fig. 26 Obstacle detection and tracking flight tests.

In a subsequent phase, real collision avoidance tests will take place. Preliminary collision avoidance tests will deal with simulated fixed obstacles to verify correct engagement of autonomous collision avoidance system. Thus, the sensing system will be bypassed.

Then, real collision avoidance tests will take place. In these tests, the flying laboratory, with all systems on, will fly several near collision trajectories with a single intruder in its field of regard. On the basis of detection and tracking system estimates, the flight control computer will generate and follow in real time a proper escape trajectory in case of predicted collision.

VII. Conclusions and Further Research

This paper presented the Autonomous Collision Avoidance System developed by the Italian Aerospace Research Center (CIRA) for its project on innovative UAV systems named TECVOL. System architecture was reported and relevant hardware and software components were described. They are based on a multiple sensor array and three real-time processing units. Using sensors based on different technologies (i.e. active microwave, passive infrared, and visible cameras) it is possible to compensate the lack of performance of single sensors. The resulting system is all-time all-weather and provides large detection range and accurate range measurements, while also offering the potential for high data rate estimates and fine angular resolution at smaller distances. The multi-sensor tracking algorithm is based on Extended Kalman filtering in Cartesian North-East-Down coordinates and Singer model for acceleration components, and was estimated to be a good compromise between tracking accuracy and reliability at very short distances, which is considered to be the worst case condition for the anti-collision system. A numerical strategy for the validation of developed algorithms was described and the relevant results were discussed. Regarding the obstacle detection and tracking phase, radar/electro-optical fusion was demonstrated to hold a dramatic improvement in tracking accuracy, besides augmenting system reliability thanks to the fact that detection for the different sensors is based on completely different physical phenomena. The estimated residual rms errors are compatible with system requirements. The effects on tracking accuracy of navigation system errors were pointed out. In summary, biases in navigation errors are almost completely filtered in body angular estimates, and thus corrupt only NED estimates. As for the collision avoidance phase, a minimum deviation control strategy was described and tested in comparison with other escape strategies (maximum command and bang-bang). The developed strategy resulted the most efficient in simulations, avoiding collisions and minimizing maximum deviation from the nominal trajectory in a 4D sense. The results shown in this paper are essentially based on detailed numerical off-line simulations but real-time hardware in the loop simulations are currently in progress and flight tests on a Very Light Aircraft (VLA) have been scheduled and will be executed in the next few months. Moreover, sensor fusion and autonomous collision avoidance algorithms will be extended to the case of multiple cooperative/non-cooperative aircrafts.

Acknowledgments

This work was supported by TECVOL, an internal CIRA project, and IFATS (Innovative Future Air Transport System) project, under contract No. AST3-CT-2004-503019-IFATS.

References

[1] Walker, J., "Safe Integration of Unmanned Aircraft Systems – UAVs into Civil Managed Airspace," *Air Traffic Control Association Congress*, Forth Worth, TX, 2nd November 2005.

[2] Okrent, M., "Civil Uav Activity within The Framework of European Commission Research," *Proceedings of AIAA 3rd Unmanned Unlimited Technical Conference*, Chicago, IL, 2004, AIAA Paper 2004-6329, pp. 1–12.

[3] Wolfe, R. C., "NASA ERAST Non-Cooperative Detect, See, & Avoid (DSA) Sensor Study," Modern Technology Solutions Inc., Alexandria, VA, September 2002.

[4] Utt, J., McCalmont, J., and Deschenes, M., "Test and Integration of a Detect and Avoid System," *Proceedings of AIAA 3rd Unmanned Unlimited Technical Conference*, Chicago, IL, 2004, AIAA Paper 2004-6329, pp. 1–10.

[5] Walker, J., and Kenagy, R., "Guidance Material and Considerations for Unmanned Aircraft Systems," Radio Technical Commission for Aeronautics (RTCA) Inc., DO-304, Washington, DC, March 2007.

[6] "Standard Specification for Design and Performance of an Airborne Sense-and-Avoid System," ASTM International, F2411-04, West Conshohocken, PA, April 2004.

[7] Shakernia, O., Chen, W. Z., Graham, S., Zvanya, J., White, A., Weingarten, N., and Raska, V. M., "Sense and Avoid (SAA) Flight Test and Lessons Learned," *2nd AIAA Infotech@Aerospace Conference and Exhibit*, Rohnert Park, CA, May 2007, Paper 2007-3003, pp. 1–12.
[8] Gibbs, D. G., "Sense and Avoid Flight Demonstration," *2nd AIAA Infotech@Aerospace Conference and Exhibit*, Rohnert Park, CA, May 2007, Paper 2007-2720, pp. 1–15.
[9] Maroney, D. R., Bolling, R. H., Athale, R., and Christiansen, A. D., "Experimentally Scoping the Range of UAS Sense and Avoid Capability," *2nd AIAA Infotech@Aerospace Conference and Exhibit*, Rohnert Park, CA, May 2007, Paper 2007-2850, pp. 1–16.
[10] Accardo, D., Moccia, A., Cimmino, G., and Paparone, L., "Performance Analysis and Design of an Obstacle Detection and Identification System," *1st AIAA Infotech@Aerospace Conference*, Arlington, VA, September 2005, Paper 2005-7175, pp. 1–18.
[11] Kuchar, J. K., and Yang, L. C., "A Review of Conflict Detection and Resolution Modelling Methods," *IEEE Transactions on Intelligent Transportation Systems*, Vol. 1, No. 4, December 2000, pp. 169–179.
[12] Fasano, G., Accardo, D., Moccia, A., and Paparone, L., "Airborne Multisensor Tracking for Autonomous Collision Avoidance," *Proceedings of IEEE 9th International Conference on Information Fusion*, Florence, Italy, July 2006, paper no. 311, pp. 1–7.
doi: org/10.1109/ICIF.2006.301724
[13] Lerro, D., and Bar-Shalom, Y., "Tracking with Debiased Consistent Converted Measurements Versus EKF," *IEEE Transactions. on Aerospace and Electronic Systems*, Vol. 29, No. 3, July 1993, pp. 1015–1022.
[14] Blackman, S. S., *Multiple-Target Tracking with Radar Applications*, Artech House, Dedham, MA, USA, 1986, pp. 101–107.
[15] Singer, R. A., Sea, R. G., and Housewright, K. B., "Derivation and Evaluation of Improved Tracking Filter for Use in Dense Multitarget Environments," *IEEE Transactions on Information Theory*, Vol. 20, No. 4, July 1974, pp. 423–432.
[16] Carbone, C., Ciniglio, U., Corraro, F., and Luongo, S., "A Novel 3D Geometric Algorithm for Aircraft Autonomous Collision Avoidance," *45th IEEE Conference on Decision and Control* (CDC'06), San Diego, CA, December 2006, pp. 1580–1585.
[17] Bilimoria, K.-D., "A Geometric Approach to Aircraft Conflict Resolution," *AIAA Guidance, Navigation, and Control Conference*, Denver, CO, August 2000, Paper 2000-4269, pp. 1–10.
[18] Skolnik, M. I., (ed.), *Radar Handbook*, McGraw Hill Professional, New York, NY, 1990, pp. 230–241.
[19] Mahafza, B. R., *Radar Systems Analysis and Design Using MATLAB*, Chapman & Hall, Boca Raton, FL, 2000, pp. 210–215.
[20] Blackman, S. S., and Popoli, R. F., *Design and Analysis of Modern Tracking Systems*, Artech House, Norwood, MA, 1999, pp. 360–372.
[21] Barfield, F., "Autonomous Collision Avoidance: The Technical Requirements," *Proceedings of the IEEE National Aerospace and Electronics Conference (NAECON),* Tip City, OH, October 2000, pp. 808–813.
[22] Swihart, D., Brannstrom, B., Griffin, E., Rosengren, R., and Doane, P., "Autonomous Collision Avoidance System for Air-to-Air Operations," *AIAA International Air and Space Symposium and Exposition: The Next 100 Years*, Dayton, OH, July 2003, Paper 2003-2755, pp. 1–10.

Tim Howard
Guest Editior